PHYSICAL REVIEW B VOLUME 45, NUMBER 7 15 FEBRUARY 1992-I

Structure-dependent weak-localization model for a superlattice

W. Szott, C. Jedrzejek,* and W. P. Kirk
Department of Physics, Texas A&M University, College Station, Texas 77843
(Received 10 June 1991)

A tight-binding theory of weak localization in the parallel and vertical conductivity of a semiconductor superlattice is presented. We take into account both the electron wave-function modulation in a superlattice and a spatial distribution of impurities in the potential barriers. These features allow us to perform realistic small-collisional-broadening calculations as quantum corrections to the Boltzmann transport. We obtain the anisotropic-elastic-scattering time, even in the case of pointlike scatterers. The anisotropy of our model differs from that considered by Bhatt, Wölfle, and Ramakrishnan. In particular, the diffusion propagator in the z direction depends on an effective diffusion constant that consists of a coherent band part and an incoherent hoppinglike part.

I. INTRODUCTION

Following the introduction of superlattices in 1970,[1] surprisingly few fundamental studies, especially of weak-localization effects, have been reported on these materials. On the other hand considerable attention has focused on investigating superlattices for applications in electronics and optics. Superlattices represent multiwell, low-barrier, strongly anisotropic three-dimensional systems, resulting from an additional periodic spatial modulation superimposed on the atomic lattice synthetically. By carefully controlling parameters such as composition, thickness, and number of layers during fabrication of superlattices, important intrinsic properties such as energy bands and effective masses can be readily modified. These circumstances provide unprecedented opportunities to study unique charge transport characteristics, which are inaccessible in other systems.

From the perspective of device applications the study of superlattices is quite important, especially for high-speed, high-mobility structures, perpendicular transport devices, sequential resonant tunneling structures, ballistic transistors, and superlattice avalanche photodetectors. A wealth of applied work now exists on superlattice applications. On the other hand, with respect to physics, only recently have several important results been obtained. Störmer *et al.*[2] observed the quantized Hall effect (QHE) and a concomitantly vanishing magnetoresistance in a GaAs/(Al,Ga)As superlattice. Less clear evidence of the QHE in CdTe/(Hg,Cd)Te has been published by Rafol, Woo, and Faurie.[3] The work of Deveaud *et al.*[4] established experimentally the existence of well-defined Bloch states along the superlattice growth axis. A positive magnetoresistance due to the suppression of antilocalization in a CdTe/(Hg,Cd)Te superlattice has been studied experimentally by Moyle, Cheung, and Ong.[5] Recently, we completed additional measurements and made extended studies of negative magnetoresistance effects in a GaAs/(Al,Ga)As superlattice.[6] The geometry of the superlattice that we studied and band calculations that we have performed indicate the existence of Bloch states in the z direction. These experimental results provide a motive for the theoretical work described below.

From here on we will use the term "superlattice" for structures that display coherent transport in the z direction. Structures that do not exhibit such a feature, like those studied by Moyle, Cheung, and Ong[5] and Englert *et al.*[7] can be analyzed, using two-dimensional (2D) theory, as a stack of independent heterojunctions.

In this paper we will be principally concerned with the weak-localization aspect of superlattice transport properties in the low collision limit. There exist few theoretical studies of classical and quantum transport in superlattices. Yang and Das Sarma[8] introduced theoretically a Bloch-type approach (as opposed to approaches that use transmission coefficients) in the calculation of vertical conductivity in superlattices. Szott, Jedrzejek, and Kirk[9] showed that the parallel conductivity has effectively a Drude form.

A desirable starting point for low magnetic field quantum corrections of transport in superlattices is three-dimensional weak-localization theory of anisotropic disordered electronic systems. A theory of negative magnetoresistance employing the restrictive assumption of an anisotropic effective mass, developed by Kawabata,[10] was not meant to be and is not applicable to superlattices as demonstrated experimentally[6] and theoretically.[9] A more general theory using an anisotropic diffusion tensor was constructed by Bhatt, Wölfle, and Ramakrishnan.[11] In addition to an anisotropic-effective-mass tensor, they also allowed the scattering amplitude to depend on direction.

Recently we introduced a weak-localization model[9] that explicitly used the band structure of a superlattice in the z direction (a similar result was also obtained by Jiang and Gong[12]). The results of this model compared favorably with the experimental results of Szott, Jedrzejek, and Kirk.[6] In the theoretical work[9] we employed two common assumptions about quantum transport in heterojunctions; namely, we assumed that there was no effect of the superlattice structure on the scattering time and that the distribution of impurities was uniform. Such approximations are considered unsatisfactory for mobility calculations.

The aim of this paper is to provide a theoretical model to interpret experiments that involve weak-localization effects in superlattices, without the restriction of a uniform impurity distribution and the absence of wave-function modulation within the superlattice. We employ, however, the simplified assumption that scattering from a single impurity is isotropic. Upon impurity averaging the effective interaction (and the lifetime) becomes anisotropic in a form that goes beyond the assumption of Bhatt, Wölfle, and Ramakrishnan,[11] which was that the scattering amplitude depended on the momentum difference between the electron final and initial state. One of our main findings is that the conductivity for superlattices still has the diffusive form [that is, the dominant contribution to the particle-particle diffusion propagator (PPDP) comes from backscattering]. We consider this an important result. However, in contrast to the result of Bhatt, Wölfle, and Ramakrishnan,[11] we have to distinguish between the diffusion coefficient $\tilde{D}_z$ that enters the classical expression for conductivity, $\sigma \propto \tilde{D}_z$, and the effective diffusion constant D_z appearing in the PPDP. The D_z we derive consists of two parts. The first part, previously derived,[9] depends on the width of the miniband. The other part has a hoppinglike character and is mostly governed by the electron wave-function modulation within the superlattice. A related work, pertaining to classical magnetoresistance in superlattices, is planned to be published elsewhere.[13]

The paper is organized as follows. In Sec. II we introduce the tight-binding Hamiltonian for a superlattice. We also calculate the impurity-averaged scattering probability W over a nonuniform impurity distribution and taking into account a wave-function modulation. This scattering probability is then used in Sec. III to derive the scattering lifetime, the particle-particle diffusion propagator, and the weak-localization correction to conductivity. In Sec. IV we present numerical results and discuss possible application of our model to the interpretation of experimental data. In the Appendix we derive analytically the parameter b characterizing scattering anisotropy.

II. TIGHT-BINDING MODEL FOR A SUPERLATTICE

A. Hamiltonian

We assume a structure in which the miniband is described by a tight-binding model. The total Hamiltonian consists of three parts:

$$H = H_0 + H_t + H_{ei} \ . \tag{1}$$

H_0 is the kinetic energy of free electrons in the planes perpendicular to the superlattice growth,

$$H_0 = \sum_{\mathbf{k}_\parallel} \sum_n \varepsilon_0(\mathbf{k}_\parallel) c^\dagger_{\mathbf{k}_\parallel,n} c_{\mathbf{k}_\parallel,n} \ , \tag{2}$$

H_t allows for tunneling,

$$H_t = \sum_{\mathbf{k}_\parallel} \sum_{n,m} t_{n,m} c^\dagger_{\mathbf{k}_\parallel,n} c_{\mathbf{k}_\parallel,m} \ , \tag{3}$$

and H_{ei} is responsible for electron-impurity scattering. $\mathbf{k}_\parallel$ is the parallel momentum in the planes and n labels the superlattice layers. The transfer along the superlattice stack is restricted to nearest neighbors. Since we assume the single-scattering approximation, we consider one impurity and then only at the end are all appropriate quantities multiplied by the number of impurities. We consider the basis functions to be the products of free waves in parallel planes and Wannier functions localized on the superlattice layers in the z direction with a period a,

$$\Psi_{\mathbf{k}_\parallel,n}(\mathbf{r},z) = \frac{1}{\sqrt{a}} f(z-na) \frac{1}{L} e^{i\mathbf{k}_\parallel \cdot \mathbf{r}} \ . \tag{4}$$

These functions constitute a complete and orthogonal set, however, they are not the eigenfunctions of $H_0 + H_t$. The eigenfunctions of $H_0 + H_t$ that are used to construct H_{ei} are the Bloch functions which will be expanded in terms of the basis functions (4).

The scattering potential is assumed to be a δ function in configuration space:

$$V_i(\mathbf{r},z) = V\delta(\mathbf{r}-\mathbf{R}_i)\delta(z-Z_i) \ . \tag{5}$$

The matrix element of this potential has the following form:

$$\langle \Psi_{\mathbf{k}_\parallel,n} | V_i | \Psi_{\mathbf{k}_\parallel+\mathbf{q}_\parallel,m} \rangle = \frac{V}{a} f^*(Z_i-na) f(Z_i-ma) \times \frac{1}{L^2} e^{i\mathbf{q}_\parallel \cdot \mathbf{R}_i} \ , \tag{6}$$

and consequently the interaction part of the Hamiltonian is

$$H_{ei} = \sum_{\mathbf{k}_\parallel,\mathbf{q}_\parallel} \sum_{n,m} \frac{V}{aL^2} f^*(Z_i-na) f(Z_i-ma) \times e^{i\mathbf{q}_\parallel \cdot \mathbf{R}_i} c^\dagger_{\mathbf{k}_\parallel,n} c_{\mathbf{k}_\parallel+\mathbf{q}_\parallel,m} + \text{H.c.} \tag{7}$$

A schematic representation of the superlattice is shown in Fig. 1. Within a tight-binding approximation the wave function specified by the impurity position Z_i is

$$f(Z_i-na) = \begin{cases} \neq 0 & \text{for } n = n_i, n_i+1 \\ = 0 & \text{otherwise} \ , \end{cases}$$

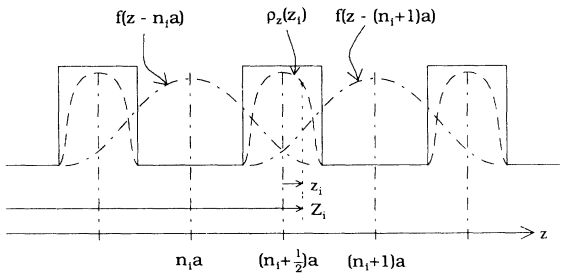

FIG. 1. Schematic representation of a superlattice. Solid line represents the bottom of conduction band (potential profile). Dashed line depicts an impurity distribution, whereas the dot-dashed line visualizes a wave function $f(z-n_ia)$. The full point refers to the z coordinate of an impurity. n_ia is the center of a potential well and $(n_i+\frac{1}{2})a$ is the center of a barrier.

where $n_i a < Z_i < (n_i+1)a$. This approximation takes into account only interlayer interactions mediated by the wave functions on the nearest-neighbor sites.

$$H_{ei}=\sum_{\mathbf{k}_\parallel,\mathbf{q}_\parallel}\sum_{n,m} V_i(n,m)e^{i\mathbf{q}_\parallel\cdot\mathbf{R}_i}c^\dagger_{\mathbf{k}_\parallel,n}c_{\mathbf{k}_\parallel+\mathbf{q}_\parallel,m}+\text{H.c.}\ , \tag{8}$$

where

$$V_i(n,m)=\frac{V}{aL^2}(|f_+|^2\delta_{n,n_i}\delta_{m,n_i}+|f_-|^2\delta_{n,n_i+1}\delta_{m,n_i+1} +f_+^* f_-\delta_{n,n_i}\delta_{m,n_i+1} +f_-^* f_+\delta_{n,n_i+1}\delta_{m,n_i})\ . \tag{9}$$

Here $f_\pm$ are defined as

$$f_\pm=f(\pm\tfrac{1}{2}a+z_i)\ , \tag{10}$$

where $z_i=Z_i-(n_i+\frac{1}{2})a$ and $|z_i|\le a/2$.

Next we Fourier transform creation and annihilation operators from the coordinate space to the momentum space in the z direction to represent H_{ei} in a basis that diagonalizes H_0+H_t, thus

$$c_{\mathbf{k}_\parallel,n}=\frac{1}{\sqrt{N}}\sum_{k_z}e^{-ik_z na}c_{\mathbf{k}_\parallel,k_z}\ , \tag{11}$$

with $k_z=2\pi l/Na$ where $l=0,1,\ldots,N-1$. This brings H_{ei} to the final form

$$H_{ei}=\sum_{\mathbf{k}_\parallel,\mathbf{q}_\parallel}\sum_{k_z,p_z} e^{i\mathbf{q}_\parallel\cdot\mathbf{R}_i}V_i(p_z,k_z)c^\dagger_{\mathbf{k}_\parallel,k_z}c_{\mathbf{k}_\parallel+\mathbf{q}_\parallel,p_z}\ , \tag{12}$$

with

$$\begin{aligned}V_i(k_z,p_z)&=\frac{1}{N}\sum_{n,m}V_i(n,m)e^{i(k_z n-p_z m)a}\\&=\frac{V}{aNL^2}e^{i(k_z-p_z)n_i a}(f_+^* f_- e^{-ik_z a}+f_-^* f_+ e^{ip_z a}+|f_+|^2+|f_-|^2 e^{i(k_z-p_z)a})\\&=\frac{V}{aNL^2}e^{i(k_z-p_z)n_i a}(f_++f_-e^{-ik_z a})^*(f_++f_-e^{-ip_z a})\ .\end{aligned} \tag{13}$$

B. Impurity averaging

We assume that the total distribution function of impurities factors into independent distributions in the parallel and z directions,

$$\rho(\mathbf{R}_i,Z_i)=\rho_\parallel(\mathbf{R}_i)\rho_z(Z_i)\ . \tag{14}$$

We use a standard uniform $\mathbf{R}$ distribution $\rho_\parallel(\mathbf{R}_i)=$const in the parallel direction. To preserve symmetry of a superlattice, a periodic z distribution $\rho_z(Z_i+na)=\rho_z(Z_i)$ is chosen. At this juncture the normalization conditions $\int d\mathbf{R}_i\rho_\parallel(\mathbf{R}_i)=\int dZ_i\rho_z(Z_i)=1$ pertain to one impurity in the system. With these assumptions for an arbitrary function that is a product of functions of parallel and perpendicular coordinates $F(\mathbf{R}_i,Z_i)=F_\parallel(\mathbf{R}_i)F_z(Z_i)$, the corresponding product factors out:

$$\langle F\rangle\equiv\int dZ_i d\mathbf{R}_i\rho(\mathbf{R}_i,Z_i)F(\mathbf{R}_i,Z_i)=\langle F_\parallel\rangle_\parallel\langle F_z\rangle_z\ . \tag{15}$$

Here the following definition of $\langle F_z\rangle_z$ is employed:

$$\begin{aligned}\langle F_z\rangle_z&=\sum_{n_i}\int_{n_i a}^{(n_i+1)a}\rho_z(Z_i)F_z(Z_i)dZ_i\\&=\sum_{n_i}\int_{-a/2}^{a/2}\rho_z(\tfrac{1}{2}a+z_i)F_z((n_i+\tfrac{1}{2})a+z_i)dz_i\ .\end{aligned} \tag{16}$$

For functions of interest within the single-impurity approximation,

$$F_z((n_i+\tfrac{1}{2})a+z_i)=F_1(n_i)F_2(z_i)\ , \tag{17}$$

and consequently

$$\langle F_z\rangle_z=\frac{1}{N}\sum_{n_i}F_1(n_i)\int_{-a/2}^{a/2}\tilde{\rho}(z_i)F_2(z_i)dz_i\ , \tag{18}$$

where $\tilde{\rho}(z_i)=N\rho_z(\frac{1}{2}a+z_i)$ is normalized in one superlattice period

$$\int_{-a/2}^{a/2}dz_i\tilde{\rho}(z_i)=1\ .$$

If $F_1(n_i)=e^{iQn_i a}$ where $Q=2\pi l/Na$, $l=0,1,\ldots,N-1$, then $(1/N)\sum_{n_i}e^{iQn_i a}=\delta_{Q,0}$. Here Umklapp processes are neglected. Similarly for $F_\parallel(\mathbf{R}_i)=e^{i\mathbf{q}_\parallel\cdot\mathbf{R}_i}$, $\langle F_\parallel\rangle_\parallel=\delta_{\mathbf{q}_\parallel,0}$.

We are now in a position to calculate the impurity-averaged scattering probability W, illustrated in Fig. 2, as

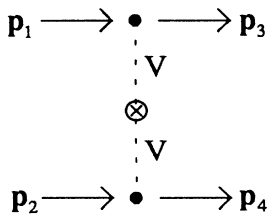

FIG. 2. A double scattering amplitude W from a single impurity ($\otimes$) with pointlike potential V. Averaging over the impurity distribution (consistent with the superlattice structure) restores momentum conservation, $\mathbf{p}_1+\mathbf{p}_2=\mathbf{p}_3+\mathbf{p}_4$.

$$W=N_{\rm imp}\langle V_i V_j\rangle_{i=j}$$
$$=\delta_{\mathbf{p}_1+\mathbf{p}_2,\mathbf{p}_3+\mathbf{p}_4}\frac{N_{\rm imp}V^2}{a^2N^2L^4}g(\mathbf{p}_1,\mathbf{p}_2,\mathbf{p}_3,\mathbf{p}_4)\ . \tag{19}$$

In the thermodynamic limit $N,L\to\infty$

$$W=\frac{n_{\rm imp}V^2}{(2\pi)^3}\delta(\mathbf{p}_1+\mathbf{p}_2-\mathbf{p}_3-\mathbf{p}_4)g(\mathbf{p}_1,\mathbf{p}_2,\mathbf{p}_3,\mathbf{p}_4)\ , \tag{20}$$

where the average impurity density is $n_{\rm imp}=N_{\rm imp}/aNL^2$.

In contrast to the isotropic 3D system, W contains an angle-dependent part

$$g(\mathbf{p}_1,\mathbf{p}_2,\mathbf{p}_3,\mathbf{p}_4)=g(p_{1z},p_{2z},p_{3z},p_{4z})$$
$$=a_1+2a_2\sum_{i=1}^{4}\cos(p_{iz}a)+2a_3\{\cos[(p_{1z}+p_{2z})a]+\cos[(p_{1z}-p_{3z})a]+\cos[(p_{1z}-p_{4z})a]\}\ . \tag{21}$$

Coefficients a_i represent various impurity averages

$$a_1=\langle f_+^4\rangle_{\tilde\rho}+\langle f_-^4\rangle_{\tilde\rho}=2\langle f_\pm^4\rangle_{\tilde\rho}\ ,$$
$$a_2=\langle f_+^3 f_-\rangle_{\tilde\rho}=\langle f_-^3 f_+\rangle_{\tilde\rho}\ , \tag{22}$$
$$a_3=\langle f_+^2 f_-^2\rangle_{\tilde\rho}\ ,$$

obtained with the use of the distribution symmetry $\tilde\rho(-z_i)=\tilde\rho(z_i)$.

III. TRANSPORT PROPERTIES

A. Scattering time

It proved to be advantageous to divide W into two parts [the momentum conserving δ function with $(2\pi)^{-3}$ omitted]:

$$W=n_{\rm imp}V^2g(p_{1z},\ldots,p_{4z})$$
$$=W_1(p_{1z}+p_{2z},p_{1z}-p_{2z},p_{3z}-p_{4z})$$
$$+W_2(p_{1z}+p_{2z},p_{1z}-p_{2z},p_{3z}-p_{4z})\ , \tag{23}$$

where

$$W_1(s,u,v)=n_{\rm imp}V^2\left[b_1(s)+b_2(s)\cos\left[\frac{ua}{2}\right]\right]$$
$$\times\left[b_1(s)+b_2(s)\cos\left[\frac{va}{2}\right]\right] \tag{24}$$

and

$$W_2(s,u,v)=n_{\rm imp}V^2b_3^2(s)\cos\left[\frac{ua}{2}\right]\cos\left[\frac{va}{2}\right]\ . \tag{25}$$

Coefficients b_i are functionals of impurity distributions:

$$b_1(s)=[a_1+2a_3\cos(sa)]^{1/2}\ ,$$
$$b_2(s)=\frac{4a_2\cos(sa/2)}{b_1(s)}\ , \tag{26}$$
$$b_3(s)=2\left[a_3-\frac{4a_2^2\cos^2(sa/2)}{b_1^2(s)}\right]^{1/2}\ .$$

We now turn to the calculation of the self-energy (see Fig. 3) which in the Born approximation reads

$$\Sigma(\mathbf{p},\varepsilon_n)=\int\frac{d^3q}{(2\pi)^3}n_{\rm imp}V^2\left\{\left[b_1(p_z+q_z)+b_2(p_z+q_z)\cos\left[\frac{a}{2}(p_z-q_z)\right]\right]^2\right.$$
$$\left.+b_3^2(p_z+q_z)\left[\cos\left[\frac{a}{2}(p_z-q_z)\right]\right]^2\right\}G_0(\mathbf{q},\varepsilon_n)\ , \tag{27}$$

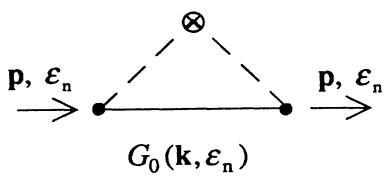

FIG. 3. The self-energy in the Born approximation.

where

$$G_0(\mathbf{q},\varepsilon_n)=\frac{1}{i\varepsilon_n-\xi_{\mathbf{q}}}\ , \tag{28}$$

and

$$\xi_{\mathbf{q}}=\varepsilon_{\mathbf{q}}-\varepsilon_F,\quad \varepsilon_{\mathbf{q}}=\varepsilon_{q_\parallel}+\varepsilon_{q_z}\ ,$$
$$\varepsilon_{q_\parallel}=\frac{\mathbf{q}_\parallel^2}{2m_\parallel},\quad \varepsilon_{q_z}=w[1-\cos(q_za)]\ . \tag{29}$$

$2w$ is the width of the miniband. Note that G_0 instead of the full Green's function is consistent with the single-impurity approximation.

Further calculations are performed for the case when the Fermi energy is greater than $2w$ (above the top of one miniband in the z direction).

The scattering lifetime τ is momentum dependent, viz.,

$$\frac{1}{\tau(\mathbf{p})}=-2\,\mathrm{Im}\Sigma(\mathbf{p},i0^+)=\frac{1}{\tau_0}[1+b\cos(p_z a)]\ , \quad (30)$$

where

$$\frac{1}{\tau_0}=\frac{2\pi g_{\parallel}(\varepsilon_F)n_{\mathrm{imp}}V^2 b_1^2(0)}{a\hbar} \quad (31)$$

and

$$b_1^2(0)=\langle(f_+^2+f_-^2)^2\rangle_{\bar{\rho}}\ ,$$
$$b=\frac{b_2(0)}{b_1(0)}=\frac{4\langle f_+^3 f_-\rangle_{\bar{\rho}}}{\langle(f_+^2+f_-^2)^2\rangle_{\bar{\rho}}}\ . \quad (32)$$

In Eq. (31) $g_{\parallel}(\varepsilon_F)$ is the projected density of states per spin, which in general reads

$$g_{\parallel}(\varepsilon,k_z)=\int\frac{d^2k_{\parallel}}{(2\pi)^2}\delta(\varepsilon-\varepsilon(k_z)-\varepsilon(\mathbf{k}_{\parallel}))$$
$$=\frac{m_{\parallel}}{2\pi\hbar^2}\Theta(\varepsilon-\varepsilon(k_z))\ . \quad (33)$$

For $\varepsilon>2w$, $g_{\parallel}(\varepsilon,k_z)=g_{\parallel}(\varepsilon)$.

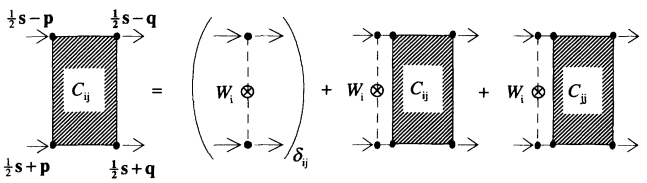

FIG. 4. Diagrammatic representation of the Bethe-Salpeter equation for the PPDP components C_{ij}.

B. Diffusion propagators

Quantum correction to the conductivity is governed by the PPDP.[14–16]

Taking advantage of the special form of the scattering probability W one can express the PPDP as the sum of four contributions:

$$C(\mathbf{s},\mathbf{p},\mathbf{q},\varepsilon_n,\omega_l)\equiv\sum_{i,j=1,2}C_{ij}(\mathbf{s},\mathbf{p},\mathbf{q},\varepsilon_n,\omega_l)\ , \quad (34)$$

where by definition

$$C_{ij}(\mathbf{s},\mathbf{p},\mathbf{q},\varepsilon_n,\omega_l)=\tilde{C}_{ij}(\mathbf{s},\varepsilon_n,\omega_l)U_i(\mathbf{s},\mathbf{p})U_j(\mathbf{s},\mathbf{q})\ . \quad (35)$$

Here

$$U_1(\mathbf{s},\mathbf{p})=b_1(s_z)+b_2(s_z)\cos(p_z a)\ , \quad (36)$$

$$U_2(\mathbf{s},\mathbf{p})=b_3(s_z)\cos(p_z a)\ . \quad (37)$$

Matrices C_{ij} and $\tilde{C}_{ij}$ satisfy the following Bethe-Salpeter equations (Fig. 4):

$$C_{ij}(\mathbf{s},\mathbf{p},\mathbf{q},\varepsilon_n,\omega_l)=n_{\mathrm{imp}}V^2U_i(\mathbf{s},\mathbf{p})U_j(\mathbf{s},\mathbf{p})\delta_{ij}+n_{\mathrm{imp}}V^2U_i(\mathbf{s},\mathbf{p})$$
$$\times\int\frac{d^3r}{(2\pi)^3}U_i(\mathbf{s},\mathbf{r})G\left[\frac{\mathbf{s}}{2}-\mathbf{r},\varepsilon_n\right]G\left[\frac{\mathbf{s}}{2}+\mathbf{r},\varepsilon_n+\omega_L\right]\sum_{k=1,2}C_{kj}(\mathbf{s},\mathbf{r},\mathbf{q},\varepsilon_n,\omega_l)\ , \quad (38)$$

$$\tilde{C}_{ij}(\mathbf{s},\varepsilon_n,\omega_l)=n_{\mathrm{imp}}V^2\delta_{ij}+n_{\mathrm{imp}}V^2\int\frac{d^3r}{(2\pi)^3}U_i(\mathbf{s},\mathbf{r})G\left[\frac{\mathbf{s}}{2}-\mathbf{r},\varepsilon_n\right]G\left[\frac{\mathbf{s}}{2}+\mathbf{r},\varepsilon_n+\omega_l\right]\sum_{k=1,2}U_k(\mathbf{s},\mathbf{r})\tilde{C}_{kj}(\mathbf{s},\varepsilon_n,\omega_l)\ , \quad (39)$$

where

$$G(\mathbf{p},\varepsilon_n)=\left[i\varepsilon_n-\xi_{\mathbf{p}}+\frac{i}{\tau(\mathbf{p})}\,\mathrm{sgn}(\varepsilon_n)\right]^{-1}\ . \quad (40)$$

If we define

$$X_{ij}(\mathbf{s},\varepsilon_n,\omega_l)=n_{\mathrm{imp}}V^2\int\frac{d^3r}{(2\pi)^3}G\left[\frac{\mathbf{s}}{2}-\mathbf{r},\varepsilon_n\right]$$
$$\times G\left[\frac{\mathbf{s}}{2}+\mathbf{r},\varepsilon_n+\omega_l\right]$$
$$\times U_i(\mathbf{s},\mathbf{r})U_j(\mathbf{s},\mathbf{r})\ , \quad (41)$$

then the solutions of the Bethe-Salpeter equations are

$$\tilde{C}_{ii}(\mathbf{s},\varepsilon_n,\omega_l)=n_{\mathrm{imp}}V^2\left[1-X_{ii}(\mathbf{s},\varepsilon_n,\omega_l)-\frac{X_{ij}^2(\mathbf{s},\varepsilon_n,\omega_l)}{1-X_{jj}(\mathbf{s},\varepsilon_n,\omega_l)}\right]^{-1}\ , \quad (42)$$

$$\tilde{C}_{ij}(\mathbf{s},\varepsilon_n,\omega_l)=\frac{X_{ij}(\mathbf{s},\varepsilon_n,\omega_l)}{1-X_{ii}(\mathbf{s},\varepsilon_n,\omega_l)}\tilde{C}_{jj}(\mathbf{s},\varepsilon_n,\omega_l)\ . \quad (43)$$

In these equations $j\neq i$. For $\varepsilon_F\gg\hbar/\tau$ and using the restriction on Matsubara frequencies (see, e.g., Ref. 17) $\varepsilon_n(\varepsilon_n+\omega_l)<0$ we get

$$\lim_{s\to 0,\omega_l\to 0^+} X_{ij}(\mathbf{s},\varepsilon_n,\omega_l)=\begin{cases}1, & i=j=1\\ 0, & i\neq j\\ \neq 1, & i=j=2\ .\end{cases} \tag{44}$$

If $X_{ij}\neq 1$ the PPDP does not have the diffusive pole. Inspection of C_{ij} leads to the conclusion that only C_{11} has a diffusive character for small s and ω_l. Other C_{ij} do contribute to transport, but behave classically with respect to change in temperature or magnetic field.

Expanding X_{ij} allows one to find diffusion constants

$$X_{11}(\mathbf{s},\varepsilon_n,\omega_l)=1-\tau_0|\omega_l|-\tau_0 D_{\parallel}\mathbf{s}_{\parallel}^2-\tau_0 D_z s_z^2\ , \tag{45}$$

where the classical diffusion constant for parallel transport, $D_{\parallel}$, has a classical form

$$D_{\parallel}=\left\langle\frac{\mathbf{v}_{\parallel}^2\tau}{2}\right\rangle_{\mathrm{FS}}=\frac{\mathbf{v}_{\parallel,F}^2\tau_0}{2}\frac{1}{(1-b^2)^{1/2}}\ . \tag{46}$$

Here we assumed that $v_{\parallel,F}\approx$const on the Fermi surface (FS) for $\varepsilon_F\gg 2w$. Diffusion constant in the z direction has more complex character

$$D_z=D_{z,c}+D_{z,h}\ . \tag{47}$$

The $D_{z,c}$ again corresponds to the classical diffusion constant

$$D_{z,c}=\langle v_z^2\tau\rangle_{\mathrm{FS}}=\frac{w^2a^2\tau_0}{\hbar^2[1+(1-b^2)]^{1/2}}\ . \tag{48}$$

The other term is the hoppinglike diffusion coefficient in the z direction,

$$D_{z,h}=\frac{a^2}{2\tau_0}\frac{P_{n,n\pm1}}{P_{n,n}+P_{n,n\pm1}}\ , \tag{49}$$

which has no classical counterpart.

Here

$$\frac{P_{n,n\pm1}}{P_{n,n}+P_{n,n\pm1}}=\frac{2\langle f_+^2 f_-^2\rangle_{\tilde{\rho}}}{\langle(f_+^2+f_-^2)^2\rangle_{\tilde{\rho}}}\ , \tag{50}$$

and $P_{n,n}$ and $P_{n,n\pm1}$ are the intralayer and interlayer scattering probabilities, respectively. The superlattice constant a is also the hopping distance (only nearest-neighbor hopping is allowed by the tight-binding nearest-neighbor model) and τ_0 is the characteristic, scattering-induced, hopping time. $D_{z,h}$ appears despite the coherent nature of weakly perturbed (quasiparticle) Bloch wave functions, and this is the main result of this work. Momentum-dependent scattering probability [see Fig. 2 and Eq. (21)] is responsible for this additional diffusion. $D_{z,h}$ formally looks like the modified one-dimensional analog of site hopping diffusion[18] (in our case this becomes hopping between adjacent layers) for which the diffusion coefficient is

$$D_{1\mathrm{D}}=\frac{a^2}{2\tau}\ . \tag{51}$$

However, in addition, the factor $P_{n,n\pm1}/(P_{n,n}+P_{n,n\pm1})$ determines the interlayer scattering probability relative to the total one which also includes the intralayer scattering as can be deduced from the form of the Hamiltonian.

Finally

$$C_{11}(\mathbf{s},\mathbf{p},\mathbf{q},\varepsilon_n,\omega_l)=\frac{\hbar}{2\pi g(\varepsilon_F)\tau_0^2}\frac{[1+b\cos(p_z a)][1+b\cos(q_z a)]}{|\omega_l|+D_{\parallel}\mathbf{s}_{\parallel}^2+D_z s_z^2}\ , \tag{52}$$

where $g(\varepsilon_F)=(1/a)g_{\parallel}(\varepsilon_F)$ for $\varepsilon_F>2w$.

C. Weak-localization correction to conductivity

Using Matsubara formalism[17] we obtain static weak-localization (WL) conductivity from the diagram in Fig. 5 as a term linear in the external frequency, viz.,

$$I_{ij}(\omega_l)=\frac{2e^2}{\beta}\sum_n\int\frac{d^3k}{(2\pi)^3}\frac{d^3q}{(2\pi)^3}v_i(\mathbf{k})v_j(\mathbf{q}-\mathbf{k})\times G(\mathbf{k},\varepsilon_n)G(\mathbf{k},\varepsilon_n+\omega_l)G(\mathbf{q}-\mathbf{k},\varepsilon_n)\times G(\mathbf{q}-\mathbf{k},\varepsilon_n+\omega_l)C(\mathbf{q},\mathbf{k},-\mathbf{k},\varepsilon_n,\omega_l)\ , \tag{53}$$

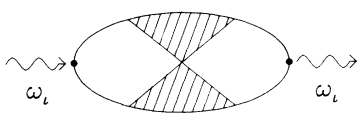

FIG. 5. Maximally crossed diagram for the weak-localization conductivity.

where the condition $\varepsilon_n(\varepsilon_n+\omega_l)<0$ of nonvanishing PPDP $C(\mathbf{q},\mathbf{k},-\mathbf{k},\varepsilon_n,\omega_l)$ is assumed. The leading term is obtained by putting $\mathbf{q}=0$ in all the factors except the PPDP which is approximated by its diffusive part,

$$C(\mathbf{q},\mathbf{k},-\mathbf{k},\varepsilon_n,\omega_l)\approx\tilde{C}_{11}(\mathbf{q},\varepsilon_n,\omega_l)b_1^2(0)[1+b\cos(k_z a)]^2\ . \tag{54}$$

Finally, we obtain the results for the parallel conductivity

$$\sigma_{\parallel,\mathrm{WL}}=-\frac{2e^2}{\pi^2\hbar}D_{\parallel}\int\frac{d^3q}{(2\pi)^3}\frac{1}{D_{\parallel}\mathbf{q}_{\parallel}^2+D_z q_z^2+\tau_{ph}^{-1}}=-\frac{e^2}{2\pi\hbar}\frac{1}{(D_z\tau_{ph})^{1/2}}\ , \tag{55}$$

and the z component of the conductivity

$$\sigma_{z,\mathrm{WL}}=\frac{D_{z,c}}{D_{\parallel}}\sigma_{\parallel,\mathrm{WL}}\ . \tag{56}$$

Here we followed the standard procedure of introducing dephasing time τ_{ph}.

It is worth noting that in the above formula the classi-

cal diffusion constant $D_{z,c}$ determines the scaling factor relating $\sigma_{z,\mathrm{WL}}$ with $\sigma_{\parallel,\mathrm{WL}}$. On the other hand, the major dependence of the WL effect on dephasing processes is governed by the full diffusion constant D_z defined in Eqs. (47)–(49).

In the standard approach, the effect of a nonzero magnetic field amounts to replacing the integral over $\mathbf{q}_\parallel$ in Eq. (55) by the sum over quantized values of $q^2_{\parallel,n}=(n+\frac{1}{2})4eB/\hbar$ and introducing the degeneracy factor $eB/(\pi\hbar)$.

IV. NUMERICAL RESULTS AND DISCUSSION

Before discussing the numerical results of our model, we comment on the assumption of the δ-function scattering potential. This approximation solely leads to unphysical results when the impurity distribution $\tilde{\rho}(z)$ approaches a δ-like profile located at the barrier centers. Physically this situation corresponds to suppression of disorder and manifests itself by infinite scattering time τ_e defined as the average of $\tau(\mathbf{p})$, Eq. (30), viz.,

$$\tau_e=\frac{\tau_0}{(1-b^2)^{1/2}} . \tag{57}$$

Inspection of Eqs. (30) and (57) shows that the divergence occurs for a factor b defined in Eq. (32) [and confined to the interval (0,1)] approaching unity. As is shown in the Appendix, Eq. (A14), the finite range of the impurity potential reduces the factor b, thus providing a finite scattering time. Consequently, we consider our model to be applicable to the systems for which the doping region thickness is greater than the range of the effective (screened) impurity potential. In contrast to metals, where the assumption of δ-function scattering potential is tolerable, the modulation-doped semiconductors call for the use of a finite-range potential. This has not been done yet in the literature, in the context of weak localization, due to formidable computational complications.

So far all the work we are aware of on weak localization is done on the semimicroscopic level. Contrary to classical theory of transport, τ_0 is not calculated but treated as a phenomenological parameter, determined from the classical conductivity. This poses a question of how the theory presented here is to be compared with experiment. Let us rewrite Eq. (31) in the form

$$\frac{1}{\tau_0}=\frac{b_1^2(0)}{\tau_0^*} , \tag{58}$$

where

$$\frac{1}{\tau_0^*}=\frac{2\pi g_\parallel(\varepsilon_F)n_{\mathrm{imp}}V^2}{a\hbar} . \tag{59}$$

One could try to use τ_0^* as a parameter and relate it, for example, to the number of impurities. However, it is common for even the best MBE samples to have mobilities 30% different for the same nominal conditions. Moreover, n_{imp} appears in combination with a poorly known potential V.

In principle, knowledge of classical conductivities $\sigma_\parallel$ and σ_z allows one to determine $D_\parallel$ and $D_{z,c}$, through the Einstein relation. Then from Eqs. (46) and (48) τ_0 and b could be found, provided the miniband width $2w$ (equivalent to the Wannier's functions overlap from adjacent layers) is known. In reality we rarely know both diffusion constants.

We decided to use τ_e as a parameter determined from $\sigma_\parallel$ or $D_\parallel$. Then the microscopic information about n_{imp} is not explicitly considered. From Eq. (57) τ_0 can be found and used in calculation of $D_{z,c}$ together with b. The disadvantage of this approach is that although τ_e depends on impurity distribution and wave-function modulation, this dependence is implicit. On the other hand, $D_{z,c}$ (as well $D_{z,h}$) contains explicit dependence on these two quantities.

Below a realistic estimate of the diffusion constants [Eqs. (48) and (49)] is given as a functional of a distribution of scattering centers (impurities). Three different impurity distributions in the superlattice growth direction are studied (in-plane or x-y distribution is assumed uniform for all cases studied here).

(a) Uniform impurity distribution across the superlattice structure. This corresponds to the background impurities and/or defects always present in semiconductor systems.

(b) Interface scattering due to interface imperfections. Here, the impurity distribution is simulated by the δ-type profile at the well-barrier junctions.

(c) In-barrier scattering. Both alloy scattering and the scattering from ionized donors are included in this category. Although the corresponding distribution function may be described by a more complicated form, only the case of a uniform profile within the barriers is examined here as an illustrative example.

The single-well approximation for the ground-state Wannier functions is used,

$$f(z)=\begin{cases} A\cos(\alpha z) & \text{for } z \text{ in the well region} \\ B\exp(\pm\beta z) & \text{for } z \text{ in the barrier region} \end{cases} \tag{60}$$

where

$$\alpha=\left[\frac{2m_\parallel E}{\hbar^2}\right]^{1/2} \tag{61}$$

and

$$\beta=\left[\frac{2m_\parallel(V_b-E)}{\hbar^2}\right]^{1/2} \tag{62}$$

are calculated for energy E of the single-well ground eigenstate (the middle of the superlattice ground miniband). Coefficients A and B are related by the continuity requirement at the interfaces. The normalization factor does not affect the results presented below. The following superlattice parameters are used: well width 18.8 nm, barrier width 3.8 nm, effective mass $m_\parallel=0.0667m_e$, Fermi energy 17.1 meV, fixed elastic scattering time $\tau_e=0.22$ ps, and barrier height V_b from 0.05 to 0.25 eV. These are typical parameters of the $GaAs/Al_xGa_{1-x}As$ superlattices measured and reported in our earlier work.[6]

Anisotropy appears in two contexts in this work. There is scattering anisotropy characterized by parameter b, where $b=0$ means no anisotropy, corresponding to $\tau_e=\tau_0$; increasing b means larger momentum dependence of $\tau(\mathbf{p})$. There is also anisotropy of the diffusion tensor. This anisotropy is mainly characterized by $2w$, the miniband width.

In Fig. 6 we show parameter b [Eq. (32)] as a function of barrier height. We see that the scattering anisotropy is significantly larger for in-barrier scattering and interface scattering than for the uniform impurity distribution. From Eq. (32) it follows that b increases with the increase of overlap of the wave functions from adjacent layers. Ever stronger dependence on barrier height (with similar tendency for the three impurity distributions) can be observed in the normalized interlayer scattering probability [Fig. (7)]: The more scatterers located closer to the barrier centers the higher the probability of interlayer hopping relative to the intralayer one. It is worth noting that the above results do not depend upon the total number (density) of scatterers which influences only the effective elastic scattering time. Figures 8(a), 8(b), and 8(c) show the results for the diffusion constants plotted versus the barrier height V_b for three different impurity distributions described in (a), (b), and (c), respectively. The parallel component of the diffusion tensor $D_{\parallel}$ is given only for comparison. The classical part of the z component, $D_{z,c}$, depends very weakly upon the type of impurity distribution discussed here. Its dependence on the barrier height is almost identical for all three distributions and is mainly determined by the exponential decrease of the superlattice miniband width $2w$ with the increasing barrier height V_b. The hopping part of the z component $D_{z,h}$ also decreases with V_b. However, the reason for this behavior lies in the strong reduction of the interlayer scattering probability for high barriers (see Fig. 7). The case (a) of uniform scattering throughout the superlattice is characterized by a very small hopping term $D_{z,h}$ compared to the classical one $D_{z,c}$ [they differ at least by a factor of 100, see Fig. 8(a)]. By contrast, the in-barrier scattering (c) reveals a significant contribution of the hopping term to the total diffusion constant D_z. The two parts are of approximately equal magnitude as shown in Fig. 8(c). The interface scattering (b) represents an intermediate sit-

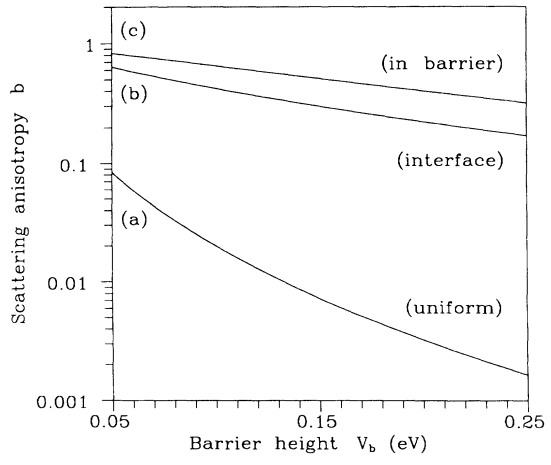

FIG. 6. Scattering anisotropy b as a function of barrier height for (a) uniform impurity distribution, (b) interface scattering, and (c) in-barrier scattering. The other superlattice parameters are well width 18.8 nm, barrier width 3.8 nm, effective electron mass $0.0667m_e$, Fermi energy 17.1 meV, elastic scattering time 0.22 ps.

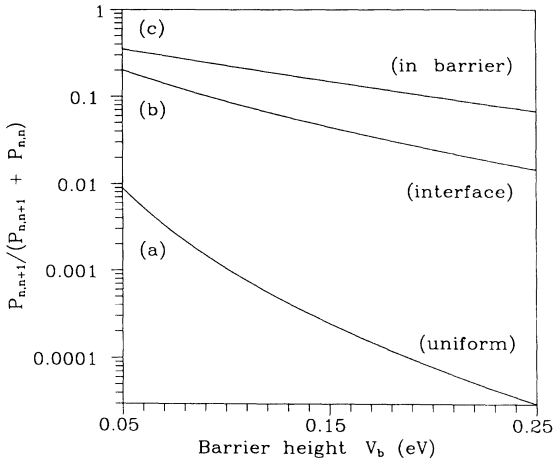

FIG. 7. Relative interlayer scattering probability in a superlattice as a function of barrier height for (a) uniform impurity distribution, (b) interface scattering, and (c) in-barrier scattering. The superlattice parameters are as in Fig. 6.

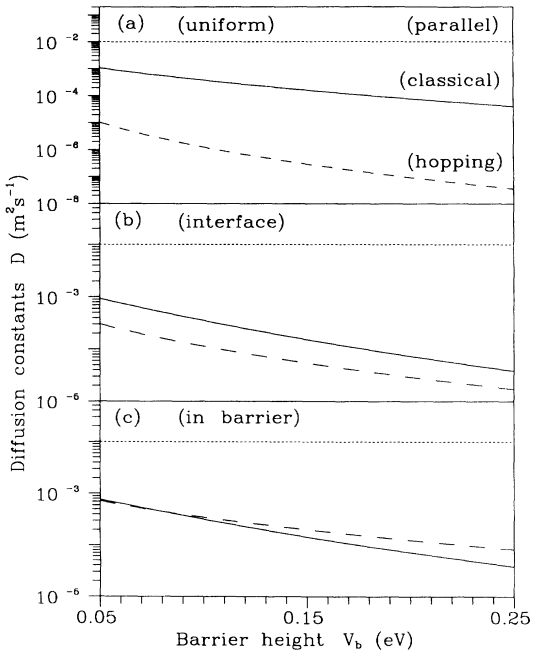

FIG. 8. Diffusion constants in a superlattice as a function of barrier height. Solid, dashed, and dotted curves represent, respectively, the classical ($D_{z,c}$), hopping ($D_{z,h}$), and parallel ($D_{\parallel}$) components of the diffusion constant. Plots (a), (b), and (c) refer to uniform scattering distribution, interface scattering, and in-barrier scattering, respectively. The superlattice parameters are as in Fig. 6.

uation. Here, $D_{z,h}$ contributes about 20% to the diffusion constant D_z. This number is almost independent of the barrier height as can be seen in Fig. 8(b). This behavior of $D_{z,h}$ for different impurity distributions is again governed by the interlayer scattering probability (Fig. 7).

The results of Fig. 8(c) require an additional comment. Our theory is based on a small-collisional-broadening-assumption,

$$\frac{\hbar}{\tau_0} \leq w \ . \tag{63}$$

Neglecting the weak impurity distribution dependence, the ratio of the hopping to coherent terms for the diffusion in the z direction is

$$\frac{D_{z,h}}{D_{z,c}} \approx \frac{\hbar^2}{\tau_0^2 w^2} \ . \tag{64}$$

Therefore, when $D_{z,h}$ becomes comparable to $D_{z,c}$, the small-collisional-broadening assumption becomes questionable. This occurs for small enough τ_0, i.e., it reflects the fact that $D_{z,h}$ is inversely proportional to τ_0. For the parameters considered here this happens for the in-barrier impurity distribution. However, for real semiconductor systems the finite range of the scattering potential effectively smoothes the impurity distribution.

As mentioned previously, the application of the present model to the interpretation of experimental data is not straightforward. Several works have recently been published (in addition to Ref. 6) in which the coherent transport (existence of Bloch wave functions) in the vertical direction is shown. The most convincing is the work of Störmer *et al.*,[2] who from the Shubnikov–de Haas data on the Fermi surface exhibiting the existence of clearly separated maximum and minimum orbits demonstrated the three-dimensionality of the electronic system in a GaAs/(Al,Ga)As superlattice. Lambert *et al.*[19] extracted diffusion coefficients from time-resolved photoluminescence measurements. They compared two kinds of samples: GaAs/$Al_xGa_{1-x}As$ thin barrier superlattice, where $x=0.3$, with $Al_yGa_{1-y}As$ reference alloy, with $y=0.15x$. These two systems have the same number of dopants. Their average diffusion coefficient increases with a decreasing period of the superlattice down to the period $L=60$ Å and then levels off at a value corresponding to the equivalent alloy. Such an isotropy in D can possibly be explained by interface roughness. Thin barrier $Al_xGa_{1-x}As$ superlattice, was also investigated by Schneider, Grahn, and von Klitzing,[20] who found direct evidence of Bloch transport. Most relevant is that mobility enhancement was observed by Ye *et al.*[21] by regular positioning of donor impurities. Weak dependence on the tilt angle (though not studied systematically) suggests weak anisotropy. However, since their measurements were performed at large magnetic fields, no direct comparison with the present theory is possible.

To summarize, the model presented in this work addresses the problem of weak-localization transport in superlattices with an emphasis on the effects of the electron wave-function modulation and impurity distribution. It is a natural expansion of the basic model derived by us in Ref. 9. Its tight-binding superlattice Hamiltonian, envelope function approximation, and arbitrary impurity distribution result in a nontrivial z-momentum dependence of the scattering probability. Consequently, anisotropy described in our model differs from that considered by the theory of Bhatt, Wölfle, and Ramakrishnan.[11] This anisotropy leads to a complicated formula for the PPDP. There exists, however, a diffusive term in it, which is responsible for weak localization. The form of this term is a standard one. The noteworthy physical effect is that the diffusion coefficient in the z direction has not only a coherent (classical) part but also an incoherent or hopping part. This process reveals some aspects that are similar to the intervalley diffusion scattering problem considered by Fukuyama.[22] The significance of the hopping-induced diffusion strongly depends on the distribution of the scattering centers with respect to the superlattice structure.

Our numerical results indicate that more theoretical work (particularly, avoiding the use of the δ-function interaction potential and considering Umklapp processes[23]) has to be done. Also thorough experimental measurements using different superlattice geometry, doping profiles, and the direction of the magnetic field in magnetoresistance have to be performed before definite answers about the nature of quantum corrections to electron transport in superlattices can be given. The extension of this work to finite-range potentials such as that used by Stern and Howard[24] is nontrivial and will be discussed in future work.

ACKNOWLEDGMENTS

Stimulating discussions with S. Das Sarma and H. Fukuyama are gratefully acknowledged. This material is based in part on work supported by the Texas Advanced Technology Program (Grant No. 3611), the Texas A&M University Board of Regents AUF-sponsored Materials Science and Engineering Program (Grant No. AUF 24424-IV), Department of Commerce–National Institute of Standards and Technology Grant No. 60NANB7D0740, and by the National Science Foundation (Grant No. DMR 88-00359). One of the authors (C.J.) acknowledges partial support from the Polish Ministry of Science, Higher Education and Technology (Projects No. CPBP 01.03 and No. RRI-14).

APPENDIX

From Eq. (57) it follows that the divergence of τ_e occurs when the factor b, as defined in Eq. (32), approaches unity. This unphysical feature can result only when the assumption of the δ-function scattering potential is used [see Eq. (5)]. Here we demonstrate that the finite range of the impurity potential reduces the factor b, thus providing a finite scattering time.

In what follows we use a more general electron-

impurity potential in separable form,

$$V_i(\mathbf{r},z)=V_{ir}(\mathbf{r})V_{iz}(z)=V_r(\mathbf{r}-\mathbf{R}_i)V_z(z-Z_i)\ , \quad \text{(A1)}$$

but we investigate only one specific doping profile. Using Eq. (A1) we get the following matrix elements (in which only the relevant z part is written):

$$\langle \Psi_n|V_i|\Psi_m\rangle \propto \int dz\ V_z(z-Z_i)f^*(z-na)f(z-ma)\ . \quad \text{(A2)}$$

Employing the tight-binding approximation with $n,m=n_i,n_i+1$ we get the following integrals:

$$\int dz\ V_z(z-z_i)f^*(z\pm\tfrac{1}{2}a)f(z\pm\tfrac{1}{2}a)\ . \quad \text{(A3)}$$

Then, in Eqs. (9) and (13) $|f_\pm|^2$ and $f_+^*f_-$ are, respectively, substituted with

$$|f_\pm|^2\rightarrow\int dz\ V_z(z-z_i)|f(z\pm\tfrac{1}{2}a)|^2\ , \quad \text{(A4)}$$

$$f_+^*f_-\rightarrow\int dz\ V_z(z-z_i)f^*(z+\tfrac{1}{2}a)f(z-\tfrac{1}{2}a)\ , \quad \text{(A5)}$$

etc. As a result, modified impurity averages a_1,a_2,a_3 are (f assumed real)

$$a_1=2\int dz_i\tilde{\rho}(z_i)\left[\int dz\ V_z(z-z_i)f^2(z\pm\tfrac{1}{2}a)\right]^2\ , \quad \text{(A6)}$$

$$a_2=\int dz_i\tilde{\rho}(z_i)\int dz_1 V_z(z_1-z_i)f^2(z_1\pm\tfrac{1}{2}a)\times\int dz_2 V_z(z_2-z_i)f(z_2+\tfrac{1}{2}a)f(z_2-\tfrac{1}{2}a)\ , \quad \text{(A7)}$$

$$a_3=\int dz_i\tilde{\rho}(z_i)\int dz_1 V_z(z_1-z_i)f^2(z_1+\tfrac{1}{2}a)\times\int dz_2 V_z(z_2-z_i)f^2(z_2-\tfrac{1}{2}a)\ . \quad \text{(A8)}$$

To investigate the case which previously led to the singularity in τ_e we assume the δ-function doping profile

$$\tilde{\rho}(z_i)=\delta(z_i)\ . \quad \text{(A9)}$$

We then obtain

$$a_1=2I_{++}^2=2I_{--}I_{++}=2I_{--}^2\ ,$$
$$a_2=I_{++}I_{+-}=I_{--}I_{+-}\ , \quad \text{(A10)}$$
$$a_3=I_{++}I_{--}\ ,$$

where

$$\left.\begin{matrix}I_{++}\\I_{--}\end{matrix}\right\}=\int dz\ V_z(z)f^2(z\pm\tfrac{1}{2}a)\ ,$$
$$I_{+-}=\int dz\ V_z(z)f(z+\tfrac{1}{2}a)f(z-\tfrac{1}{2}a)\ . \quad \text{(A11)}$$

Consequently

$$b=\frac{4a_2}{a_1+2a_3}=\frac{I_{+-}}{I_{++}}\ . \quad \text{(A12)}$$

Using the same approximation for the wave functions in the barriers as before [see Eq. (60)], and assuming a simple potential which retains the main feature of interest (finite range)

$$V_z(z)=\begin{cases}V & \text{for } |z|<r/2\\ 0 & \text{for } |z|>r/2\ ,\end{cases} \quad \text{(A13)}$$

we get the final result for b,

$$b=\frac{\beta r}{\sinh(\beta r)}\ . \quad \text{(A14)}$$

For $r\rightarrow 0$ $b=1$, while $b<1$ for finite range r.

*Permanant address: Department of Physics, Jagellonian University, Cracow, Poland.

[1]L. Esaki and R. Tsu, IBM J. Res. Dev. **14**, 61 (1970).
[2]H. L. Störmer, J. P. Eisenstein, A. C. Gossard, W. Wiegmann, and K. Baldwin, Phys. Rev. Lett. **56**, 85 (1986).
[3]S. Rafol, K. C. Woo, and J. P. Faurie, in *Proceedings of 18th International Conference on the Physics of Semiconductors*, edited by O. Engström (World Scientific, Singapore, 1987), p. 773.
[4]B. Deveaud, J. Shah, T. C. Damen, B. Lambert, and A. Regreny, Phys. Rev. Lett. **58**, 2582 (1987).
[5]J. K. Moyle, J. T. Cheung, and N. P. Ong, Phys. Rev. B **35**, 5639 (1987).
[6]W. Szott, C. Jedrzejek, and W. P. Kirk, Phys. Rev. Lett. **63**, 1980 (1989).
[7]T. Englert, J. C. Maan, G. Remenyi, H. Künzel, K. Ploog, A. Fischer, and A. Briggs, Surf. Sci. **142**, 68 (1984).
[8]S.-R. Eric Yang and S. Das Sarma, Phys. Rev. B **37**, 10090 (1988).
[9]W. Szott, C. Jedrzejek, and W. P. Kirk, Phys. Rev. B **40**, 1790 (1989).
[10]A. Kawabata, J. Phys. Soc. Jpn. **49**, 628 (1981).
[11]R. N. Bhatt, P. Wölfle, and T. V. Ramakrishnan, Phys. Rev. B **32**, 569 (1985).
[12]Q. Jiang and C. D. Gong, J. Phys. Condens. Matter **1**, 9413 (1989); Phys. Lett. A **127**, 105 (1988).
[13]W. Szott, C. Jedrzejek, and W. P. Kirk (unpublished).
[14]B. L. Altshuler, D. E. Khmel'nitskii, A. L. Larkin, and P. A. Lee, Phys. Rev. B **22**, 5142 (1980).
[15]P. Lee and T. V. Ramakrishnan, Rev. Mod. Phys. **57**, 287 (1985).
[16]H. Fukuyama, in *Electron-Electron Interactions in Disordered Systems*, edited by A. L. Efros and M. Pollak (North-Holland, Amsterdam, 1985), p. 155.
[17]G. D. Mahan, *Many-Particle Physics* (Plenum, New York, 1981).
[18]J. D. Doll and A. F. Voter, Annu. Rev. Phys. Chem. **38**, 413 (1987).
[19]B. Lambert, B. Deveaud, A. Chomette, F. Clerot, and A. Regreny, Surf. Sci. **228**, 446 (1990).

[20]H. Schneider, H. Grahn, and K. von Klitzing, Surf. Sci. **228**, 362 (1990).
[21]Q. Ye, A. Zrenner, F. Koch, H. Sigg, D. Heitmann, and K. Ploog, Surf. Sci. **228**, 453 (1990).
[22]H. Fukuyama, J. Phys. Soc. Jpn. **50**, 3652 (1981); Suppl. Prog. Theor. Phys. **69**, 221 (1980).
[23]N. Wiser, Contemp. Phys. **25**, 211 (1984).
[24]F. Stern and W. E. Howard, Phys. Rev. **163**, 816 (1967).